Femtosecond time-resolved study of the generation and propagation of phonon polaritons in $LiNbO_3$

P. C. M. Planken, L. D. Noordam, J. T. M. Kennis, and A. Lagendijk
FOM–Institute for Atomic and Molecular Physics, Kruislaan 407, 1098 SJ Amsterdam, The Netherlands
(Received 26 August 1991)

Using intense femtosecond pulses, we have generated phonon polaritons in the ferroelectric crystal $LiNbO_3$. Phonon-polariton pulses consisting of ≈ 8 oscillations of the electric field were generated. They were detected in a time-resolved way by diffraction of a probe pulse from the standing wave formed by these phonon polaritons. We determined their dispersion for frequencies up to 130 cm^{-1}. The pulse width of the phonon polaritons was ≈ 3 ps. In addition, we have studied their propagation in the crystal, by diffracting a probe pulse from one of the traveling phonon polaritons. We demonstrate that in this case, the diffracted signal is sensitive to the phase of the phonon polariton. Analytical calculations show that this can be explained in terms of the interference between the electric fields of the nondiffracted probe beam and the first-order diffracted probe beam.

I. INTRODUCTION

In noncentrosymmetric crystals such as $LiNbO_3$, $BaTiO_3$, and $LiTaO_3$, there are transverse optical (TO) -phonon branches that are infrared active and Raman active. TO phonons typically absorb light at particular frequencies in an interval ranging from 10 to 1000 cm^{-1}. Whenever electromagnetic waves of approximately the same frequency and wave number as a TO phonon propagate through such a crystal, they will couple with these mechanical vibrations to form a new mixed excitation: a phonon polariton.[1,2] In the frequency region ω_p and wave-vector region $\mathbf{q}$ where the coupling is strongest, a phonon polariton has both photon character and phonon character. The dispersion $\omega_p(\mathbf{q})$ then strongly deviates from both the dispersion of the uncoupled TO phonon and the uncoupled electromagnetic wave.

Phonon polaritons can be used to study the dielectric properties of the crystal in which they were generated. They can also be used for the generation of far-infrared light. There are several nonlinear optical processes in crystals that can be used to generate far-infrared light. One of them is $\chi^{(2)}$ difference-frequency generation where a beam at frequency ω_1 is mixed with a beam at ω_2 and their difference frequency $\omega_1-\omega_2$ is generated. When the frequency of the far-infrared light lies in the neighborhood of a TO-phonon frequency, the $\chi^{(3)}$ of the medium becomes important too. Another, similar, method is to use difference-frequency generation within the bandwidth of an ultrashort laser pulse.[3] Stimulated Raman scattering was used to generate tunable nanosecond far-infrared light in $LiNbO_3$,[4] and also to generate phonon polaritons in NH_4Cl (Ref. 5) using picosecond pulses. In the latter experiment, their propagation was studied by scattering a probe pulse from the propagating phonon polariton. Nearly forward Raman scattering is the technique mostly used to study the dispersion of phonon polaritons in crystals such as $LiNbO_3$,[6–9] $LiTaO_3$,[10] and $BaTiO_3$.[11,12]

In the last decade, lasers providing femtosecond pulses have proven to be a valuable tool in experiments designed to generate far-infrared pulses. One of these techniques is optical rectification. Optical rectification is a second-order nonlinear optical process where a dc polarization proportional to the envelope of an ultrashort laser pulse is generated. It was demonstrated that, with this method, ultrashort electrical pulses consisting of approximately one oscillation of the electric field could be generated in $LiTaO_3$.[13,14] It was shown that the technique could be used to coherently excite phonon polaritons in $LiTaO_3$.[15] In fact, if far-infrared light is generated with a frequency close to the TO-phonon frequency, the light propagates as a phonon polariton. The generation of these ultrashort electrical pulses using femtosecond pulses can be viewed as the $\chi^{(2)}$ equivalent of impulsive stimulated Raman scattering.[16,17] With impulsive stimulated Raman scattering, femtosecond pulses are used to coherently excite a molecular vibration[18] or a sound wave.[19] This is, for example, done by creating a spatially periodic standing-wave grating in a medium with two overlapping ultrashort pump pulses. If the pump pulses are shorter than one period of oscillation of the Raman-active vibration, they coherently excite the vibration. From the grating, a delayed probe pulse is diffracted and the diffraction efficiency is measured as a function of the delay between the pump pair and the probe. The vibration can be detected in a time-resolved way, because the pulses are shorter than one period of oscillation of the excited vibration.

Phonon polaritons can propagate with a group velocity, $d\omega/dk$. The propagation of phonon polaritons is interesting because it potentially allows the study of the damping as a function of distance. This was demonstrated by Gale, Vallée, and Flytzanis in a crystal of NH_4Cl.[5] They used Raman scattering with picosecond pulses to scatter light from a traveling polariton at ≈ 1300 cm^{-1} and determined the dephasing as a function of distance. Clearly, their pulses were much longer then one period of oscillation of the polariton. Auston and Nuss studied propagation of phonon polaritons in a crystal of $LiTaO_3$ by measuring the wave form of the electric field, generat-

ed with optical rectification, as a function of distance.[13] They made use of the linear electro-optic effect to detect the change in the polarization of a probe pulse induced by the electric field of the phonon polariton.

Here we are interested in studying phonon-polariton generation and propagation in $LiNbO_3$ in a time-resolved way by diffracting a probe pulse from a pump-induced refractive-index grating as will be explained in the next section. The use of femtosecond pulses in the study of phonon polaritons offers considerable advantages compared to studies where picosecond, nanosecond, or cw lasers are used. The bandwidth of femtosecond pulses is very large so that far-infrared phonon-polariton frequencies can be made by mixing frequency components within the bandwidth of these pulses. With femtosecond pulses, much higher laser intensities can be used in the crystal before damage occurs. We will show that the consequence of this is that ultrashort coherent phonon polaritons can be created and detected very efficiently in $LiNbO_3$. Note that for high frequencies, femtosecond pulses are needed to observe the oscillations of the phonon polariton in a time-resolved way.

In addition, we performed experiments focused on the propagation of these phonon polaritons. Surprising results are found when a femtosecond probe pulse is diffracted from a *propagating* phonon-polariton refractive-index grating. In this case, the diffracted signal is sensitive to the phase of the phonon polariton. This can only be measured with pulses that are shorter than one period of oscillation of the phonon polariton. The technique that we used to generate phonon polaritons in $LiNbO_3$ is similar to that recently used by Etchepare *et al.* to excite phonon polaritons in $PbTiO_3$.[20]

The paper is organized as follows. In the next section we will describe the experimental setup used for the generation of phonon polaritons. We then show some results concerning the generation of phonon polaritons and their dispersion. Roughly the second half of this paper is devoted to the study of their propagation. We show the result of diffraction of a probe pulse from a propagating grating followed finally by a calculation explaining the result.

II. EXPERIMENTAL

The experimental setup is based on an amplified short pulse laser system. Femtosecond pulses with central wavelength 620 nm from a colliding-pulse mode-locked laser (CPM) are amplified to an energy of approximately 250 μJ at a 10-Hz repetition rate. Dispersion increases the pulse duration when they propagate through the dye amplifiers and the optical components. Self-phase modulation generates a somewhat larger bandwidth. For this reason, the pulses are led through a folded two-prism compressor to shorten their duration. Approximately 30 μJ is used for the experiment. The beam is first spatially filtered to obtain a good beam profile. In this way, the amount of amplified spontaneous emission is also reduced to approximately 5%. After spatial filtering, we have an energy of several microjoules per pulse. The pulse duration, measured with autocorrelation using second harmonic generation in a short potassium dihydrogen phosphate crystal, was found to be ≤ 100 fs. The beam is split into three beams as shown in Fig. 1 where the pump-probe setup is depicted schematically. Two beams form the pump-pulse excitation pair. They are aligned parallel to each other with distance d. Using a lens with a focal length f of typically 25 cm, the beams are focused through a pinhole with an appropriate diameter to optimize spatial overlap in the focus. The third beam is the probe beam. It passes through a computer controlled variable-delay line, which has an accuracy of 1 μm. 1% of the probe beam is split off, using a CaF_2 window and is detected by a Si diode. It is used as the reference signal. The beam is aligned parallel with respect to the pump pair but in a different horizontal plane so that we are able to spatially separate the signals caused by self-diffraction[21] of the pump beams, from the diffracted probe beam after the focus. The probe is focused through the pinhole with the same lens as the pump pair.

Temporal overlap between the two pump pulses is found by first replacing the pinhole by a $50\times10\times1$ mm^3 (or a $10\times10\times3$ mm^3) polished $LiNbO_3$ and varying the delay between the pump pulses until self-diffraction[21] is observed. Temporal overlap between the probe pulse and the pump pair is found by delaying the probe pulse with respect to the pump pair until diffraction of the probe pulse from the pump grating is observed. The first-order diffracted probe beam is detected with the help of a Si diode. The signals from the reference diode and the diode used for the detection of the diffracted probe pulse are fed into the computer. A typical experiment consists of several computer controlled delay scans, each scan consisting of 70 delay positions. At each delay position, 20 laser shots are collected. The diode signals for each laser shot, together with the delay position, are stored on floppy disk for later analysis.

The focused pump pair creates a spatially periodic intensity grating in the crystal. Frequency components within the bandwidth of the pulses are mixed using the $\chi^{(2)}$ and the $\chi^{(3)}$, to generate phonon polaritons with frequency ω_p and wave vector $\pm\mathbf{q}$. Note that phase matching is important since only those frequencies will be

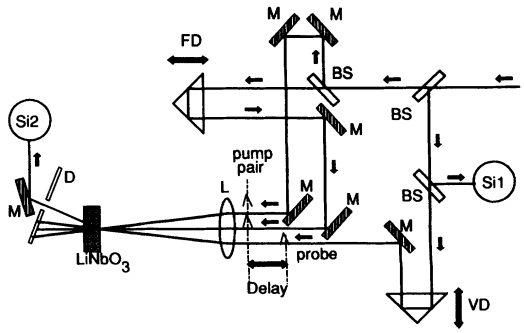

FIG. 1. Experimental setup for the generation of phonon polaritons. M, Mirrors coated for maximum reflection at 620 nm; FD, fixed delay; VD, variable delay; L, lens; BS, beamsplitters; Si1 and Si2, silicon diodes; and D, diaphragm.

amplified which "fit" the imposed wave vector $\mathbf{q}$. The absolute value $|\mathbf{q}|$ of the wave vector is determined by the pump vacuum wavelength λ_{pu}, and the angle γ between the two pump pulses. For small angles we can write $\gamma \approx d/f$, with d the separation between the pump beams. If $\mathbf{k}_1$ and $\mathbf{k}_2$ are the wave vectors of the two pump pulses, then the length of the wave vector $\mathbf{q}$ can be expressed as[21]

$$q \equiv |\mathbf{q}| = |\mathbf{k}_1 - \mathbf{k}_2| = 2\pi d/\lambda_{\mathrm{pu}} f \ . \tag{1}$$

A different value of q can be chosen by changing d or f.

The c axis of the crystal is chosen parallel to the polarization of the laser. In this configuration, both the laser pulses and the generated phonon polaritons are of pure extraordinary character and thus only the largest electro-optic coefficient (r_{33}) is relevant. Because the two pump pulses are identical, *two* counter propagating phonon polaritons are created that form a standing wave. The standing wave modulates the index of refraction through the linear electro-optic effect and thus forms a periodically vanishing grating. The grating can be detected in a time-resolved way by diffracting a probe pulse from it. Results are described in the next section.

III. GENERATION AND DETECTION OF PHONON POLARITONS IN $LiNbO_3$

A. Diffraction efficiency versus pump-probe delay

We monitor the energy of one of the first-order diffracted probe beams. A typical measurement of the diffraction efficiency of the pump grating as a function of delay between pump pair and probe pulse is shown in Fig. 2. Starting at small negative delays, the diffracted signal increases rapidly until it reaches a maximum at delay zero (here the signal is flat due to saturation of the detector). The diffracted signal at delay zero is completely dominated by diffraction caused by effects other than the presence of phonon polaritons, such as the electronic

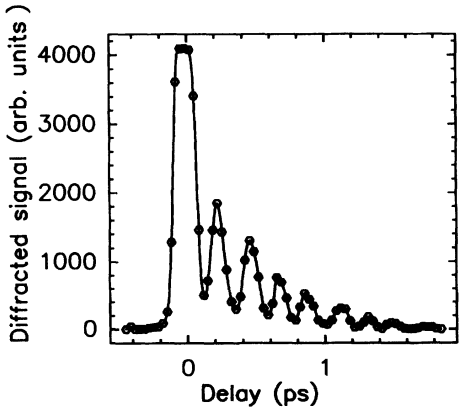

FIG. 2. Measured first-order diffracted signal as a function of delay between pump pair and probe, for $q = 2513 \pm 100$ rad cm^{-1}. The signal oscillates at twice the frequency of the polariton. Note that the signal at delay zero is very large due to other contributions to the diffracted signal such as the electronic $\chi^{(3)}$ of the medium.

$\chi^{(3)}$ of the crystal. For positive delays, the signal oscillates at twice the frequency of the phonon polariton $2\omega_p$ because we have created *two* counter propagating phonon polaritons, each with frequency ω_p, that form a standing wave. It is interesting that we can resolve the oscillations of the grating in a time-resolved way. This is because the pulse duration of the 620-nm pulses is shorter than the period of oscillation of the phonon polariton: We are studying the response of the medium in the impulsive limit.[16,17]

We can get an estimate of the value of the electric field of the generated polariton from the following. The diffraction efficiency η_{dif} of a refractive-index grating, is given by[21]

$$\eta_{\mathrm{dif}} \equiv I_1/I_{\mathrm{in}} = \left[\frac{\pi \Delta n_e \, l}{\lambda_{\mathrm{pu}}} \right]^2 , \tag{2}$$

with I_1 the intensity of the first-order diffracted beam, I_{in} the intensity of the probe beam before the crystal. Δn_e the induced extraordinary refractive index change, l the thickness of the grating, and λ_{pu} the pump-laser wavelength. A typical value of the diffraction efficiency that we measured at the first maximum after delay zero, was $\eta_{\mathrm{dif}} = 1.0 \times 10^{-3}$. If we take the following experimental parameters: $l = 1$ mm, $\lambda_{\mathrm{pu}} = 620$ nm, then the pump-pair-induced refractive-index change that we calculate from Eq. (2) is $\Delta n_e = 6 \times 10^{-6}$. If we assume that, by means of the electro-optic effect, the index of refraction is modulated only by the presence of the electric field associated with the (photonlike) phonon polariton, we can calculate the electric field strength.[23] The electric field is polarized along the c axis of the crystal and propagates in the x direction. The equation relating the relevant electro-optic coefficient r_{33}, the index of refraction n_e, the induced index of refraction *change* Δn_e, and the electric field $|\mathcal{E}|$ is given by[23]

$$|\mathcal{E}| = \frac{2 \Delta n_e}{n_e^3 r_{33}} \ . \tag{3}$$

If we use the numbers $r_{33} = 30.8 \times 10^{-12}$ m/V, $n_e = 2.2$, $\Delta n_e = 6 \times 10^{-6}$, we calculate an electric-field strength of $|\mathcal{E}| \approx 4 \times 10^4$ V/m. This number is on the order of field strengths generated with optical rectification.[13]

B. Dispersion of phonon polariton

By forcing a q value onto the system and measuring the frequency of ω_p, the dispersion relation $\omega_p(q)$ can be determined. The results are shown in Fig. 3. The figure shows that for frequencies lower than ≈ 50 cm^{-1}, the frequency is linear in wave vector q. This is the photonlike regime of the phonon polariton. The deviation from linearity for higher frequencies is indicative of the fact that the phonon polariton begins to increase its phonon character there. The dispersion $\omega_p(q)$ can also be calculated. In $LiNbO_3$ there are four infrared-active TO phonons for polarizations parallel to the c axis.[22] These phonons all influence the dielectric constant $\epsilon(\omega_p)$ and consequently the dispersion $\omega_p(q)$. If we assume that these

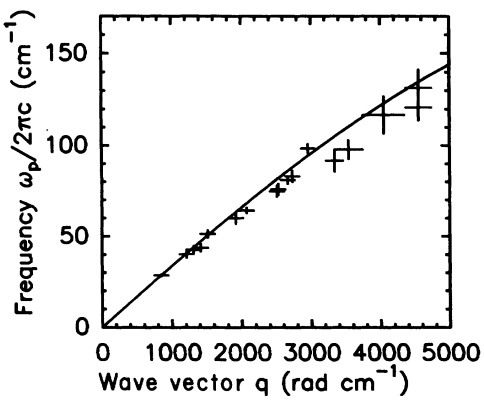

FIG. 3. Measured phonon-polariton dispersion in $LiNbO_3$. The curve is calculated using reflectivity data of Ref. 22 and contains no adjustable parameters. The agreement with the measured points is good.

TO-phonon branches are independent, then we can simply add their contributions to the dielectric constant. If we also assume that we can neglect phonon damping, then we can write for the dielectric constant

$$\epsilon(\omega_p)=\epsilon_{\rm el}+\sum_{i=1}^{4}\frac{\epsilon_{{\rm st},i}\omega_{T,i}^2}{\omega_{T,i}^2-\omega_p^2}\ , \tag{4}$$

with $\epsilon_{{\rm st},i}$ the contribution to the static dielectric constant $\epsilon(\omega_p=0)$ of TO phonon branch i, with frequency $\omega_{T,i}$, and with $\epsilon_{\rm el}$ the electronic dielectric constant. The expressions for the dispersion relation reads[2,22]

$$q^2-\frac{\omega_p^2}{c^2}\epsilon_{\rm el}-\sum_{i=1}^{4}\frac{\omega_p^2}{c^2}\frac{\epsilon_{{\rm st},i}\omega_{T,i}^2}{\omega_{T,i}^2-\omega_p^2}=0\ . \tag{5}$$

The strength $\epsilon_{{\rm st},i}$ of each mode can be deduced from reflectivity measurements and these numbers are well known for the case of $LiNbO_3$. We use the data of Barker and Loudon[22] and reproduce their results in Table I. The curve in Fig. 3 is calculated from Eq. (5) using the data from Table I and contains therefore no adjustable parameters. The agreement with the measured points is good. It should be noted that the contribution to the dispersion of the lowest 248-cm^{-1} mode is by far the largest in this frequency range and that the incorporation of the other modes only leads to a small correction of the calculated curve.

In Fig. 3, the deviation of the measured points from a straight line $\omega_p/2\pi c \propto q$ for high frequencies, is a sure sign that the phonon polariton begins to increase its phonon character there, while for low frequencies, it is dominated by electromagnetic wavelike behavior.

TABLE I. Room-temperature central frequencies, linewidths, and absorption strengths of the four TO phonons in $LiNbO_3$ polarized parallel to the c axis (Ref. 22).

i	TO phonon frequency (cm^{-1})	Linewidth (cm^{-1})	$\epsilon_{{\rm st},i}$
1	248	21	16.0
2	274	14	1.0
3	307	25	0.16
4	628	34	2.55

The generated frequencies range from 30 to 130 cm^{-1}. It proved to be very difficult to resolve signals with a frequency higher than 130 cm^{-1}. Although we did observe decaying signals for large q vectors, the amplitude of the oscillating part of the signal was too small so that we were not able to measure the frequency. There may be two reasons for this: (i) For the highest frequencies, the time resolution of the setup decreases due to the fact that the pump-pulse duration becomes of the order of the period of the phonon polariton. This leads to a smearing out of the signal. This is another way of saying that the frequency bandwidth of the pump pulse puts a maximum on the value of the phonon-polariton frequency that can be generated. (ii) For the higher frequencies, we need larger q values and, consequently, larger angles of γ. Because the length of the pump pulses in the crystal is short compared to the focus diameter, large values of γ will lead to reduced effective-overlap area. This results in a lower diffraction efficiency. With these pulses we can therefore not measure the dispersion for large values of the wave vector q. If one is not interested in time-resolved experiments, however, the dispersion can be measured with Raman scattering, as was demonstrated with nanosecond pulses.[4]

In optical rectification (the Čerenkov-type experiment), it is also the duration of the femtosecond pump pulse that is one of the limiting factors that determines the length and the frequency bandwidth of the generated electrical pulse.[13–15]

The number of oscillations of the phonon polariton depends on the ratio of the grating spacing and the diameter of the pump beams in the focus. The diameter of the focus clearly also determines the width of the polariton. This resembles the Čerenkov-like experiment where, in order to generate electrical pulses that have a width that is only determined by the bandwidth of the laser pulse, the diameter of the focus in the crystal must be very small.

The frequency of the generated phonon polariton with respect to that of the lowest frequency transverse-optical phonon determines whether the $\chi^{(3)}$ process becomes important in the generation process. If the frequency is much lower than that of the TO phonon, then there is almost no energy in the phonon part of the phonon polariton. In that case, the process is the far-infrared equivalent of $\chi^{(2)}$ difference-frequency generation. The other extreme is when the frequency of the phonon polariton is close to the TO-phonon frequency. Now, a large fraction of the energy resides in the phonon part and the $\chi^{(3)}$ *is* important. The generation process is now a combination of parametric generation and Raman scattering[24] and is therefore different from pure Raman scattering processes where *only* the $\chi^{(3)}$ has a nonzero value. In our case we generate frequencies ≤ 130 cm^{-1}, whereas 248 cm^{-1} is the frequency of the lowest TO phonon. The generation process is therefore mainly (but not totally) a $\chi^{(2)}$ process.

The use of femtosecond pulses is an advantage if one wants to generate high electric-field strengths, because the damage threshold I_{dam} of a material increases when shorter pulses are used: $I_{dam} \propto \tau^{-1/2}$. Using parameters, typical of our experiment, beam diameter $D=1.5$ mm, focal length $f=25$ cm, pump-pair wavelength 620 nm, pulse duration $\tau=100$ fs, energy per pulse $E=2$ μJ, we arrive at an intensity in the focus of the pump pair of ≈ 40 GW/cm^2. At this intensity, no visible damage occurred. At the highest intensities ($>10^{11}$ W/cm^2), the diffracted signal was obscured by stray light emerging from the crystal, roughly in the shape of a cone, occasionally accompanied by visible damage.

A related point deserves some attention. $LiNbO_3$ is an insulator with an optical bandgap of ≈ 4.0 eV (310 nm). Using 620 nm as the excitation pulse, two-photon absorption will occur and charge carriers will be excited to the conduction band of the material. Charge carriers are accelerated by the electric fields of the femtosecond pump pulse and could damage the crystal. However, as indicated above, this did not seem to play an important role. Moreover, within an accuracy of 5%, we did not observe any absorption. This becomes radically different for energies of around 20 μJ where strong absorption *was* seen. Due to the fact that two-photon absorption is a nonlinear process, this seemingly sharp transition within one order of magnitude variation of intensity should not be surprising.

IV. PHONON-POLARITON PROPAGATION

A. Introduction

The standing-wave phonon polariton is formed by two counterpropagating waves that leave the focus. For a traveling wave, there is no such thing as a periodically vanishing grating. If carefully aligned, however, then for fixed delay, the probe pulse will see a grating which appears to be frozen. This is true because, during propagation of the probe pulse, the traveling wave will also propagate which causes the probe pulse to see always the same phase of the traveling wave. For a different but fixed delay, some other part of the frozen wave will be sampled, and we expect to see a diffracted signal with a different energy. Intuitively, it would seem that, since the grating does not vanish periodically, the diffracted signal as a function of delay between the probe and the traveling wave will be a smooth curve. This smooth curve is then expected to have roughly a Gaussian shape where each point on the curve reflects the number of "grating lines" in the focus at a given delay, and therefore the diffraction efficiency.

B. Experimental

The setup used for the detection of the traveling waves is identical to that of the measurements where we detect the standing wave. The experiment begins by measuring the diffraction from the standing wave. With respect to the pump pair, we then give the probe beam a small displacement in the horizontal plane in which the phonon-polariton waves propagate. The displacement in the focus is of the order of one to several pump-focus diameters so that the pump and the probe are separated. The distance between the center of the pump and the center of the probe in the focus is measured by scanning a pinhole through the focus and monitoring the transmission. With the crystal in the focus, we then place a photodiode at a considerable distance behind the crystal, at the position where the first-order diffracted signal was observed when all three beams spatially overlapped. Note that the displacement of the probe with respect to the pump may cause the diffracted signal to arrive at a point that is somewhat displaced with respect to the position of the detector.

The measured signal is weak compared to the signal that we measure when pump pair and probe spatially overlap, and is usually not visible to the naked eye. This is probably caused by the decay of the phonon polariton while it propagates and/or by its divergence, since both mechanisms will lead to a decreasing electric-field strength, therefore a weaker grating and consequently a lower diffraction efficiency. In these experiments we increased the diameter of the probe beam before the focusing lens, thereby decreasing its diameter in the focus. This leads to a higher probe intensity in the focus.

C. Diffraction from a propagating phonon polariton: Results

A measurement of the diffracted signal versus delay for a distance between pump pair and probe of ≈ 80 μm, is given in Fig. 4. The signal shows, contrary to our intuition, an oscillatory curve under a Gaussian-like envelope of ≈ 3 ps duration, with oscillations at approximately the frequency of the polariton, *not* twice the frequency. Approximately eight oscillations are visible. The signal is the result of a measurement series, consisting of 20 laser shots at each delay position. When these measurements are repeated, the results are qualitatively the same. The

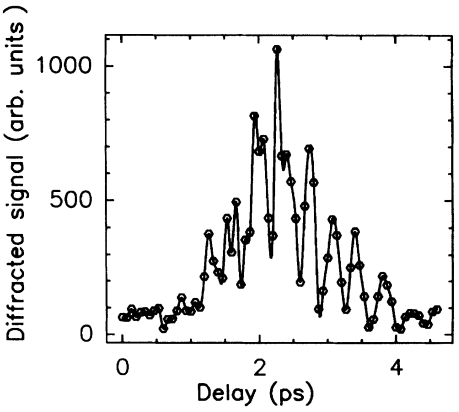

FIG. 4. Measured diffracted signal (points) vs delay between probe pulse and phonon polariton. The signal oscillates at approximately the frequency of the polariton, not twice the frequency. We choose a wave vector $\mathbf{q}=2335\pm100$ rad cm^{-1} measured at a frequency of 85 ± 5 cm^{-1}. The curve is a guide to the eye.

oscillations, however, are phase shifted with respect to the previous series or they show oscillations that show a phase jump within the same series. When the different series are added, the oscillations are smeared out and the signal begins to look more and more like its envelope. If the signal is sensitive to the phase of the phonon polariton, then it becomes clear why the signal smears out after the addition of several measurement series: The phase of the phonon polariton is determined by the phase difference between the two pump pulses. Since we are not interferometrically stable over times much longer then the time needed to complete one measurement series (1–2 min), the phase difference between the two pump pulses changes and, consequently, the phase of the phonon polariton changes too. At this point it is important to emphasize the following: We see individual oscillations of the phonon polariton. The modulation depth is high. The signal appears to be sensitive to the phase of the phonon polariton.

D. Diffraction from a refractive-index grating: Calculations

The fact that we measure an oscillatory signal can be explained at least qualitatively: The traveling wave creates a refractive-index grating (phase grating) with a Gaussian envelope by means of the linear electro-optic effect. From this grating we diffract a probe pulse which has a Gaussian spatial profile in the direction perpendicular to its propagation direction. We assume that the probe propagates in the z direction, perpendicular to the grating. For simplicity, we also assume that both the spatial profile of the probe and the grating only vary with coordinate x. We then basically have a two-dimensional problem.

For a given delay between grating and probe, the problem then reduces to that of diffraction of a probe beam from a static grating. In doing this we also ignore the fact that we are in reality diffracting light from a moving grating which has a momentum associated with it. The grating actually shifts the frequency of the diffracted light with a value that corresponds with the frequency of the grating. This shift is in our case *always* smaller than the bandwidth of our pulses. We are now in a position to calculate the diffracted signal for a certain diffraction angle α as a function of the delay between the probe and the grating. Note that, in solving this problem, the time dependence enters the calculation implicitly through the delay between the grating and the probe. The calculation is based on similar calculations in Ref. 25.

For the electric field of the phonon polariton we take a pulse with a cosine oscillation under a Gaussian envelope. The effects of the phase grating are then taken into account by means of the phase transmission factor

$$T=\exp(i\{1+t\exp[-(x-x')^2/x_1^2]\times\cos[2\pi(x-x')/a]\}) , \quad (6)$$

with t the amplitude of the phase change, x' the shift (delay) of the maximum of the envelope of the phase grating with respect to the spatial maximum of the probe field, x_1 proportional to the spatial width of the phase grating, and $2\pi/a=|\mathbf{q}|$ the wave vector of the grating. The calculation uses the position x' as the "delay" variable. At the end of the calculation this will be translated into a time delay.

Since both the cosine term and the Gaussian term in Eq. (6) contain the argument $(x-x')$, we implicitly assume that the point where the phase change has a maximum coincides with the maximum of the Gaussian.

We can estimate the typical value of t from the average phase change that the probe accumulates while it propagates through the region of the crystal where the presence of the phonon polariton changes the index of refraction. The accumulated phase change $\Delta\phi$ is

$$\Delta\phi\approx\omega\,\Delta n_e\, l/c , \quad (7)$$

with ω the probe frequency, Δn_e the induced extraordinary refractive-index change, l the crystal or grating thickness, and c the velocity of light. Using typical numbers $\omega=3.0\times10^{15}$ rad/s, $\Delta n_e=1.0\times10^{-6}$, $l=3.0\times10^{-3}$ m, and $c=3.0\times10^{8}$ m/s, we calculate a phase change of $\Delta\phi\approx3.0\times10^{-2}$ rad. The calculation serves to illustrate that $\Delta\Phi\ll1$, for the 3-mm-thick crystal and consequently also for the 1-mm crystal. Note that the number for the induced refractive-index change Δn_e is typical only for measurements where pump pair and probe spatially overlap. It is much smaller for the propagating polariton outside the focus, since it was already noted that the diffracted beam was usually not visible to the naked eye. We now have $t\ll1$, allowing us to approximate Eq. (6) by a Taylor series and truncate after the second term[25] so that we have

$$T\approx\exp(\{1+it\exp[-(x-x')^2/x_1^2]\times\cos[2\pi(x-x')/a]\}), \text{ for } t\ll1 . \quad (8)$$

The probe beam that propagates in the z direction has a spatial x dependence of the electric field amplitude according to

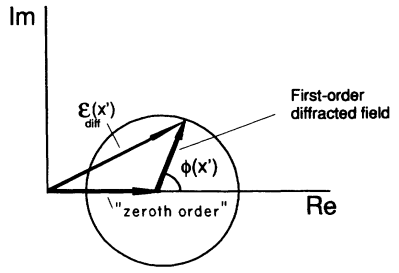

FIG. 5. Total electric-field amplitude for fixed α. The vector that corresponds to the first-order diffracted signal has an oscillating phase $\Phi(x')$ that is translated into an amplitude oscillation of the total electric-field amplitude $\mathcal{E}_{dif}(x')$ when the vector is displaced along the real axis by the "zeroth-order" contribution (or along any direction, for that matter).

$$\mathcal{E}_{\text{probe}} \propto e^{-x^2/x_0^2} . \tag{9}$$

The diffracted field amplitude $\mathcal{E}_{\text{dif}}(\alpha)$ as a function of diffraction angle α can then be calculated, from Ref. 25

$$\mathcal{E}_{\text{dif}}(\alpha) \propto \int_{-\infty}^{+\infty} e^{ik\alpha x} T e^{-x^2/x_0^2} dx . \tag{10}$$

This integral can easily be calculated and reads

$$\begin{aligned}\mathcal{E}_{\text{dif}}(\alpha) \propto\ & x_0\sqrt{\pi}\, e^{-k^2\alpha^2 x_0^2/4} \\ & + \frac{it}{2} x_0 x_1 \left[\frac{\pi}{x_1^2+x_0^2}\right]^{1/2} \exp\left\{\left[-\left[\frac{2\pi}{a}+k\alpha\right]^2 - \frac{4x'^2}{x_0^2 x_1^2} + i4x'\left[\frac{k\alpha}{x_1^2}-\frac{2\pi}{ax_0^2}\right]\right] \Big/ 4\left[\frac{1}{x_0^2}+\frac{1}{x_1^2}\right]\right\} \\ & + \frac{it}{2} x_0 x_1 \left[\frac{\pi}{x_1^2+x_0^2}\right]^{1/2} \exp\left\{\left[-\left[\frac{2\pi}{a}-k\alpha\right]^2 - \frac{4x'^2}{x_0^2 x_1^2} + i4x'\left[\frac{k\alpha}{x_1^2}+\frac{2\pi}{ax_0^2}\right]\right] \Big/ 4\left[\frac{1}{x_0^2}+\frac{1}{x_1^2}\right]\right\} .\end{aligned} \tag{11}$$

In this derivation we have omitted the prefactor containing terms like $r_0^{-1/2}$, with r_0 the distance between the grating and the detector, which ensure that the electric-field strength and therefore the intensity decreases when the distance increases.

This awesome-looking solution (11) actually has a rather simple physical explanation. The solution is the sum of three terms. The first contains no grating parameters and is the original probe field as it diverges (diffracts) due to the final diameter of the beam in the focus. The two other terms are the first-order diffracted beams on the left- and right-hand sides of the probe beam. They peak for diffraction angles $\alpha = -2\pi/(ka)$ and $\alpha = +2\pi/(ka)$, respectively. There are no higher-order diffracted beams due to the assumption that $t \ll 1$. Each of the first-order diffracted electric fields can be represented by a vector in the complex plane with a phase $\Phi(x')$,

$$\Phi(x') = \frac{\pi}{2} + x'\left[\frac{k\alpha}{x_1^2} \pm \frac{2\pi}{ax_0^2}\right] \Big/ \left[\frac{1}{x_0^2}+\frac{1}{x_1^2}\right] \tag{12}$$

that changes when x' is varied, but that has an amplitude that decreases monotonically. When we now add the complex vector of the first term (which is real), we actually displace the rotating vector along the real axis as can be seen from Fig. 5. The amplitude of this vector sum has now become a periodic function of x' (note that a value for x' corresponds to a particular delay between probe and grating). Since intensity is proportional to $|\mathcal{E}|^2$, the diffracted signal as a function of x' will show oscillatory behavior.

What we have described is in fact the interference between the "zeroth-order" probe field and the first-order diffracted probe field. The effect becomes important when the electric-field amplitudes of both contributions are approximately the same. The value of α for which this is the case will lie somewhere between the maxima of both contributions, as is shown in Fig. 6. Note that we implicitly assumed that the contribution to the diffracted field for values of α where the interference is the greatest has only two sources: the "zeroth-order" field and *only* the first-order diffracted field that peaks for these values of α. The contribution from the other first-order diffracted field can clearly be neglected. The figure shows the calculated value for the diffracted intensity as a function of diffraction angle α. In this figure, the x' was given the value 6 μm to clearly show the dip in the intensity for a value of α where the electric-field strengths are approximately the same. The intensity around these values of α oscillates as a function of x'. The "spatial period" of this oscillation Λ_{osc} is not precisely the period of the grating a. Λ_{osc} can be obtained from Eq. (12) and reads

$$\Lambda_{\text{osc}} = \frac{2\pi(1/x_0^2+1/x_1^2)}{(k\alpha/x_1^2 \mp 2\pi/ax_0^2)} . \tag{13}$$

For $x_1 \to \infty$, we get $\Lambda_{\text{osc}} \to a$.

The difference between a and Λ_{osc}, for finite values of x', can be appreciated from the following example where we use the same parameters as in Fig. 6. We consider the

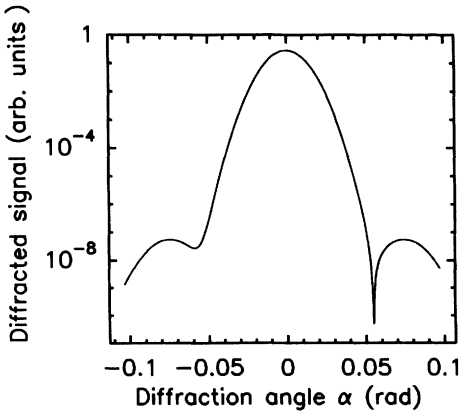

FIG. 6. Calculated diffracted intensity as a function of α. The figure clearly shows the interference dip between the "zeroth-order" and the first-order contribution. The magnitude of this dip oscillates as a function of x'. Values for the different parameters: $x_0 = 30$ μm, $x_1 = 60$ μm, $a = 23.8$ μm, $k = 3.5 \times 10^6$ m^{-1}, $x' = 6$ μm, $t = 0.001$.

+ case in Eq. (13): If we take $x_1=60$ μm, $x_0=30$ μm, $k=3.5\times10^6$ m^{-1}, $a=23.8$ μm, and $\alpha=0.057$ rad, we calculate $\Lambda_{osc}=25$ μm. This difference with a can be neglected due to the uncertainty in the frequency of the phonon polariton deduced from the measurement in Fig. 4. In Fig. 7 the diffracted intensity is plotted versus delay $t_d=x'n_p/c$ for a value of α where oscillations in the intensity are expected. Here n_p is the index of refraction for the propagating wave, and c is the speed of light in vacuum. All the other parameters have the same values as in Fig. 6. This calculated curve should be compared with the measured signal plotted in Fig. 4. It can be seen that many of the essential features are reproduced. We therefore conclude that the model used to explain the oscillations is a realistic one.

In the Čerenkov-like experiments in $LiTaO_3$, the phase and amplitude of the propagating broadband electrical pulse is measured by the value of the polarization change of a CPM probe pulse, induced by the propagating electrical pulse.[13–15] This technique is clearly capable of determining accurately both the phase and the amplitude of the electrical pulse.

In our case, we measure the propagation of phonon polaritons, which have a well-defined frequency and a well-defined wave vector, by scattering a probe pulse from the induced grating. Although in our experiment we are sensitive to the phase of the phonon polariton, it is difficult to determine its value.

At this point the following should be noted. We have ignored the frequency shift that occurs when light is diffracted from the grating. The interference between the diffracted field and the zeroth-order contribution was based on the assumption that both fields have the same central frequency. We know that this is not fully correct because of the frequency shift of the diffracted field. However, as was pointed out in the beginning of the section, the frequency shift is smaller than the bandwidth of the 620-nm pulses. The addition of two electric fields with a different frequency will lead to a modulation of the pulses in the time domain. This modulation period is longer than the pulse duration when the frequency difference is smaller than the bandwidth of the pulses. Consequently, our calculated results will not be affected very much by the frequency difference.

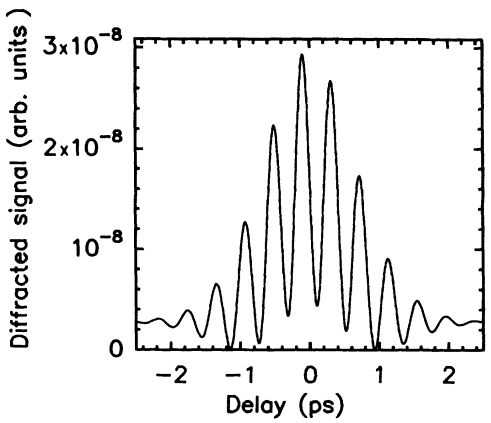

FIG. 7. Calculated density of the diffracted signal vs delay for a propagating phonon polariton. The curve shows oscillations with a period of 0.4 ps. Parameters are the same as in Fig. 6.

V. CONCLUSIONS

We have generated phonon polaritons in $LiNbO_3$, and measured their dispersion and their propagation in a time-resolved way. For the propagating case we observe oscillations in the diffracted signal versus delay that can be explained in terms of interference between the electric field of the undiffracted probe and the electric field of the first-order diffracted probe. The phonon polaritons have a duration of approximately 3 ps corresponding with an average number of oscillations of eight and an electric-field strength of several hundred V/cm.

ACKNOWLEDGMENTS

It is a pleasure to acknowledge experimental support by Bart Broers in the preliminary stage of this work and helpful discussions with Huib Bakker and Harm-Geert Muller. The work described in this paper is part of the research program of the Stichting voor Fundamenteel Onderzoek van de Materie (Foundation for Fundamental Research on Matter) and was made possible by financial support from the Nederlandse Organisatie voor Wetenschappelijk Onderzoek (Netherlands Organization for the Advancement of Research).

[1]C. Kittel, *Introduction to Solid State Physics,* 6th ed. (Wiley, New York, 1986).
[2]M. Schubert and B. Wilhelmi, *Nonlinear Optics and Quantum Electronics* (Wiley, New York, 1986).
[3]Y. R. Shen, *The Principles of Nonlinear Optics* (Wiley, New York, 1984).
[4]J. M. Yarborough, S. S. Sussmann, H. E. Purhoff, R. H. Pantell, and B. C. Johnson, Appl. Phys. Lett. **15**, 102 (1969).
[5]G. M. Gale, F. Valleé, and C. Flytzanis, Phys. Rev. Lett. **57**, 1867 (1986).
[6]M. Posledovich, F. X. Winter, G. Borstel, and R. Claus, Phys. Status Solidi **55**, 711 (1973).
[7]R. Claus and F. X. Winter, in *Polaritons,* edited by E. Burstein and F. De Martini (Pergamon, New York, 1974).
[8]M. Rokni, L. S. Wall, E. Amzallag, and T. S. Chang, Solid State Commun. **10**, 103 (1972).
[9]S. Kojima and T. Nakamura, Ferroelectrics **37**, 677 (1981).
[10]T. S. Chang, B. C. Johnson, E. Amzallag, R. H. Pantell, M. Rokni, and L. S. Wall, Opt. Commun. **4**, 72 (1971).
[11]L. Laughman, L. W. Davis, and T. Nakamura, Phys. Rev. B **6**, 3322 (1972).
[12]A. Chaves, P. Da R. Andrade, R. S. Katiyar, and S. P. S. Porto, in *Polaritons,* edited by E. Burstein and F. De Martini (Pergamon, New York, 1974).
[13]D. H. Auston and M. C. Nuss, IEEE J. Quantum Electron. **24**, 184 (1988).
[14]B. B. Hu, X.-C. Zhang, D. H. Auston, and P. R. Smith, Appl. Phys. Lett. **56**, 506 (1990).
[15]K. P. Cheung and D. H. Auston, Phys. Rev. Lett. **55**, 2152 (1985).

[16]Y.-X. Yan and K. A. Nelson, J. Chem. Phys. **87**, 6240 (1987).
[17]Y.-X. Yan and K. A. Nelson, J. Chem. Phys. **87**, 6257 (1987).
[18]S. Ruhman, A. G. Joly, and K. A. Nelson, J. Chem. Phys. **86**, 6563 (1987).
[19]K. A. Nelson, R. J. D. Miller, D. R. Lutz, and M. D. Fayer, J. Appl. Phys. **53**, 1144 (1982).
[20]J. Etchepara, G. Grillon, A. Antonetti, J. C. Loulergue, M. D. Fontana, and G. E. Kugel, in *Ultrafast Phenomena VII,* edited by C. B. Harris, E. P. Ippen, G. A. Mourou, and A. H. Zewail (Springer, Berlin, 1990).
[21]H. J. Eichler, P. Günter, and D. W. Pohl, *Laser-Induced Dynamic Gratings* (Springer, Berlin, 1986).
[22]A. S. Barker, Jr., and R. Loudon, Phys. Rev. **158**, 433 (1967).
[23]A. Yariv and P. Yeh, *Optical Waves in Crystals* (Wiley, New York, 1984).
[24]D. N. Klyshko, *Photons and Nonlinear Optics* (Gordon and Breach, New York, 1988).
[25]D. Marcuse, *Light Transmission Optics* (Van Nostrand Reinhold, New York, 1982).

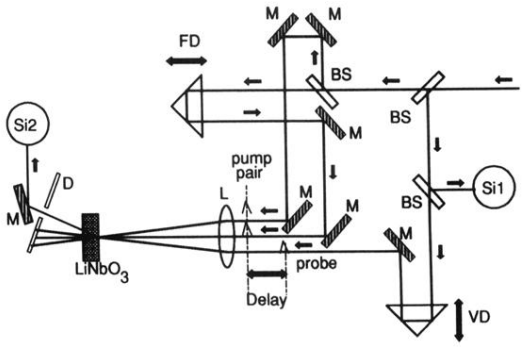

FIG. 1. Experimental setup for the generation of phonon polaritons. M, Mirrors coated for maximum reflection at 620 nm; FD, fixed delay; VD, variable delay; L, lens; BS, beamsplitters; Si1 and Si2, silicon diodes; and D, diaphragm.